Korean J. Chem. Eng., **26**(2), 576-581 (2009)

Effects of carbon on the sulfidation and hydrodesulfurization of CoMo hydrating catalysts

Hui Ge*,, Xuekuan Li*, Zhangfeng Qin*, Feixue Liang*, and Jianguo Wang*,†**

*State Key Laboratory of Coal Conversion, Institute of Coal Chemistry, Chinese Academy of Sciences, P.O. Box 165, Taiyuan, Shanxi 030001, China
**College of Chemistry and Chemical Engineering, Taiyuan University of Technology, Taiyuan 030024, China
(*Received 28 July 2008 • accepted 15 October 2008*)

Abstract−The effects of carbon addition on CoMo catalyst performance for sulfidation and hydrodesulfurization (HDS) were investigated. The carbon-containing catalyst was prepared by impregnation of γ-Al_2O_3 support with NH_3 aqueous solution containing $Co(NO_3)_2 \cdot 6H_2O$, $(NH_4)_6Mo_7O_{24} \cdot 4H_2O$ and ethylenediamine. The results indicated that the incorporation of proper carbon on CoMo catalyst can improve its HDS performance. The carbon species on the catalyst were characterized by temperature-programmed oxidation and reduction, temperature-programmed desorption of ammonia and ultraviolet-visible diffuse reflectance spectra. Two forms of carbon species were differentiated: one is spread over the catalyst surface, similar to coke formed from reaction; the other interacts with active phase as an intermediate support. The carbon species acting as intermediate support may decrease the interaction of active metals with support, which enhances the sulfidation and HDS activities of CoMo catalyst.

Key words: Hydrodesulfurization, Sulfidation, Carbon Addition, Hydrotreating Catalyst, Ethylenediamine

INTRODUCTION

The legislative specifications for ultra low sulfur transport fuels demand hydrotreating catalysts with high hydrodesulfurization (HDS) performance [1,2]. Molybdenum or tungsten sulfides supported on alumina and promoted by cobalt or nickel are typical HDS catalysts in industry [3,4]. The commercial HDS catalyst is usually available in an oxide form and a sulfiding process is then needed to transform it to sulfide form before use. The sulfidation and HDS activities of the hydrotreating catalyst are influenced strongly by the carbon species loaded on the catalyst [5].

The effects of carbon on HDS catalysts have been controversial for many years. It has been recognized in practice that the sulfidation of an HDS catalyst in the presence of oil feed is more efficient than the sulfidation in gas-phase without oil feed. Hallie [6] found that the HDS activity for a vacuum gas oil over CoMo catalyst can be enhanced by using dimethydisulfide instead of H_2/H_2S as sulfiding agent. Preda Silvy et al. [7,8] found that butanethiol was one of the most efficient sulfiding agents for model reactions (thiophene HDS and cyclohexene hydrogenation). Chianelli et al. [9] ascribed these catalytic enhancements by organosulfide as sulfiding agent to the formation of carbide-like species on the active phase surface. Recently, Wen et al. showed by density functional theory (DFT) that the carbonization of MoS_x is thermodynamically favored [10]. When using organosulfides instead of H_2S as sulfiding agent, however, Texier et al. found no significant difference in catalyst performance for HDS of dibenzothiophene and 4,6-dimethyldibenzothiophene [11]; the beneficial effect of organosulfides may just dilute the exothermicity of the oxide-sulfide transformation.

Carbon can improve the support interaction and dispersion of active phase. Active carbon-supported Co(Ni)Mo catalysts exhibit higher activity in HDS than the alumina supported counterparts [12-15]. Glasson et al. observed a positive influence of carbon species on thiophene and crude oil desulfurization over the carbon-containing $CoMo/Al_2O_3$ catalysts [16]; the carbon deposit may isolate sulfide particles from each other to maintain a high dispersion of active phase. Alonso et al. prepared unsupported carbon-containing (Co) MoS_2 with alkyl substituted ammonium thiomolybdate [17,18]. They found that the carbon species confine the active phase to small crystallites and modify the edge of MoS_2 crystallites to form carbide-like structures. These may enhance the activity of hydrotreating catalyst [19].

The controversy relative to the effects of carbon on the hydrotreating catalyst originates from the complication of carbon species in HDS catalysts; several carbon species may be simultaneously present on the catalyst surface. Therefore, in this work, carbon-containing CoMo catalysts were prepared by using ethylenediamine (EN) as carbon precursor, and various characterizations were performed to differentiate the carbon species. The effects of carbon addition on CoMo catalyst performance for sulfidation and HDS were investigated.

EXPERIMENTAL

1. Catalyst Preparation

γ-Al_2O_3 was co-impregnated with an aqueous NH_3 solution of $(NH_4)_6Mo_7O_{24}$, $Co(NO_3)_2$ and EN, followed by drying at 110 °C over night and calcination at 450 °C in N_2 for 3 h. Catalysts with the mole ratios of EN/Co=1, 1.5 and 2 were designated as CoMo(C1), CoMo (C1.5) and CoMo(C2), respectively. For comparison, a catalyst signed as CoMo(C0) was prepared in the similar way as CoMo(C1.5), ex-

†To whom correspondence should be addressed.
E-mail: iccjgw@sxicc.ac.cn
‡This work was presented at the 7th China-Korea Workshop on Clean Energy Technology held at Taiyuan, Shanxi, China, June 26-28, 2008.

cept that the subsequent calcination was performed in air. All catalysts contained 16.0 wt% MoO_3 and 3.1 wt% CoO.

2. Catalyst Characterization

Temperature-programmed oxidation (TPO) and reduction (TPR) were conducted in a quartz micro-reactor. For TPO, about 100 mg of catalyst sample was heated from room temperature to 500 °C at a rate of 5 °C/min in a stream of 5 mol% O_2 in Ar with a flow rate of 50 ml/min. CO and CO_2 in the effluent were detected by a Omni-Star 200 quadrupole mass spectrometer. For TPR, about 100 mg of sample was heated from room temperature to 850 °C at a rate of 10 °C/min and kept at this temperature for 30 min in a stream of 10 mol% H_2 in Ar with a flow rate of 25 ml/min. H_2 consumption was measured with a thermal conductive detector (TCD).

Ultraviolet-visible diffuse reflectance spectroscopy (UV-Vis DRS) was performed on a Varian Cary300 UV-Vis spectrophotometer.

The acidity of catalyst was measured by temperature programmed desorption of ammonia (NH_3-TPD) in a TP-5000 quartz micro reactor (Tianjing-Xianquan, China). About 100 mg of catalyst sample was pretreated at 500 °C for 2 h in an Ar flow of 50 ml/min, cooled down to 120 °C. Then it was saturated with dry ammonia through pulse-injection. The sample was flushed further with the Ar flow at 120 °C for 1 h to remove any physically adsorbed ammonia. After that, the sample was heated from 120 °C to 500 °C at a heating rate of 10 °C/min and the amount of NH_3 desorbed was measured with the TCD.

3. Sulfidation and HDS Tests

The sulfidation and HDS tests were performed in a fixed bed tubular flow reactor with an inner diameter of 6 mm. For the catalyst sulfidation, about 1.0 g of catalyst sample (20-40 mesh) was sulfided by a sulfiding feed of 0.1 wt% thiophene dissolved in a desulfurized and hydrogenated C6 solvent in an H_2 flow under 1.2 MPa, 290 °C, liquid hourly space velocity (LHSV) of 8.6 h^{-1}, and H_2/oil volume ratio of 140. During the sulfidation, thiophene conversion in the effluent was determined with a gas chromatograph (Shimadzu 9A) equipped with an FID detector. To examine the influence of olefins and N-containing compounds on the sulfidation, a solution of 5 wt% cyclohexene (or 0.01 wt% pyridine) and 0.1 wt% thiophene in C6 solvent was used as the sulfiding feed; the conversion of cyclohexene was determined by bromine number coulometric titration with an LC-4 micro coulometer (Luoyang-Shuangyang, China) [20].

For HDS tests, about 1.0 g of catalyst sample was first sulfided by 4.5 vol% H_2S in H_2 with a flow rate of 33 ml/min at 1.2 MPa and 400 °C for 2 h. Then the reactor was cooled to 290 °C and the FCC naphtha containing 866 ppm sulfur was introduced. The HDS reaction was carried out at 1.2 MPa, 290 °C, LHSV of 8.6 h^{-1} and H_2/oil volume ratio of 140. To ensure a steady-state operation was achieved, sampling was made after reaction lasted for at least 9 h. Sulfur content in the effluent oil was then determined with the LC-4 micro coulometer [21].

RESULTS AND DISCUSSION

1. TPO

The evolution of CO and CO_2 produced during TPO of various catalysts is shown in Fig. 1. CoMo(C1) and CoMo(C1.5) exhibit similar profiles for CO and CO_2, while CoMo(C2) presents more

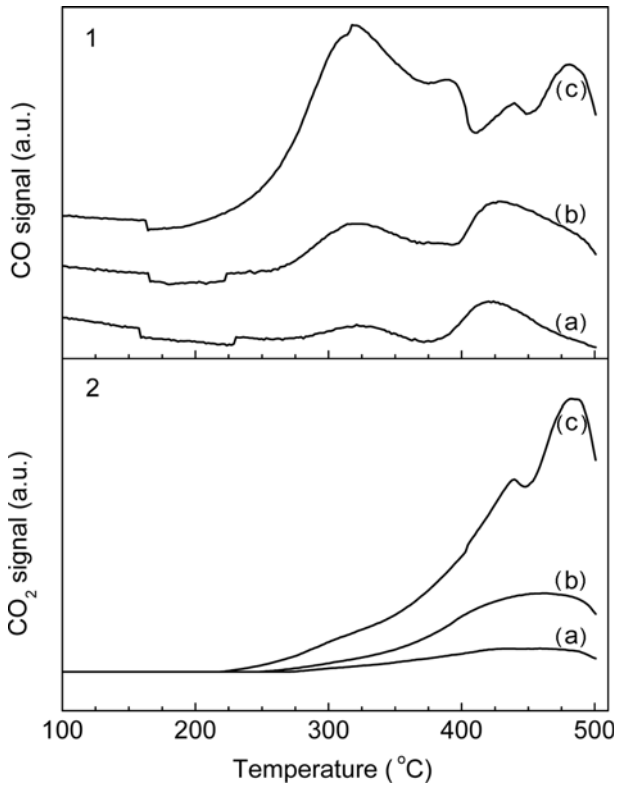

Fig. 1. TPO profiles of (a) CoMo(C1), (b) CoMo(C1.5) and (c) CoMo(C2): upper, CO evolution; lower, CO_2 evolution.

shoulder peaks. The peak area increases with carbon loading in the catalyst. CO evolution exhibits two main peaks at around 330 °C and 420 °C, respectively, while CO_2 evolution only shows one main peak at about 450 °C. The carbon deposit corresponding to low temperature oxidation may be attributed to the coke-like carbon, and the carbon species oxidized at high temperature can be attributed to the carbon species as intermediate support [16]. The former carbon species stays on the catalyst surface and is easy to oxidize; the latter carbon species is located between the active metal and sup-

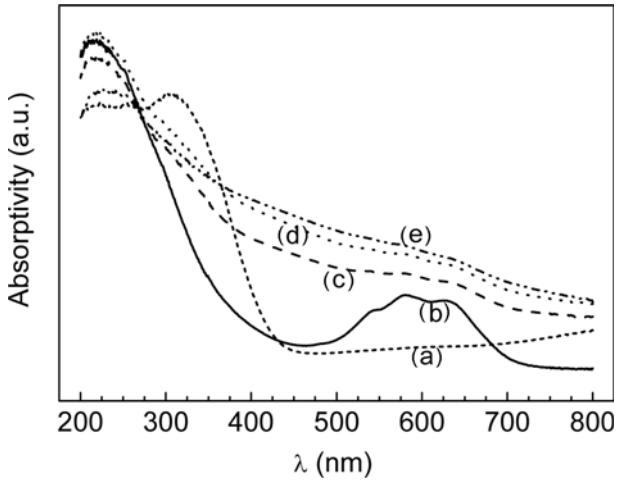

Fig. 2. UV-vis DRS of (a) MoO_3, (b) CoMo(C0), (c) CoMo(C1), (d) CoMo(C1.5) and (e) CoMo(C2).

port and needs higher temperature for its combustion. The appearance of shoulder peaks in catalyst CoMo(C2) may suggest a more complicated distribution of carbon species.

2. UV-vis DRS

The UV-vis DRS of MoO_3 and various catalysts are illustrated in Fig. 2. The triple band at about 600 nm is attributed to tetrahedral Co^{2+}, which presumably indicates the presence of the catalytically inactive $CoAl_2O_4$ [22]. This triplet area decreases in the order of CoMo(C0), CoMo(C1), CoMo(C1.5) and to CoMo(C2). Because the carbon precursor EN coordinates with Co^{2+} during impregnation, carbon species deposit around Co^{2+} upon calcination and inhibit the formation of $CoAl_2O_4$. These are favorable for Co^{2+} ions to form CoMoS active phase during sulfidation. However, it should be noted that carbon species may also cover the surface of Co^{2+} ions and prevent Co^{2+} ions from combining with MoS_2 phase.

The DRS in the region of 200-400 nm for the supported Mo species demonstrates that MoO_3 crystal is not present on the catalyst surface. The bands at 220-250 nm are attributed to the tetrahedral molybdate, whereas the band at 320 nm is assigned to the Mo-O-Mo bridge bond of the octahedral coordination [23,24]. The broad band at 280-400 nm for CoMo catalysts indicates that both the tetrahedral and octahedral molybdates are present on the support. However, a higher fraction of octahedral molybdate is present in carbon-containing catalysts than that in carbon-free catalyst.

3. TPR

H_2 consumption during TPR reflects the reducibility of molybdenum oxide; the contribution from CoO can be negligible [25]. As shown in Fig. 3, the peak around 481 ºC is due to the partial reduction of polymolybdate-like species (octahedral Mo), i.e., Mo^{6+} to Mo^{4+}. The peak at higher temperature (850 ºC) represents the reduction of polymolybdate and tetrahedrally coordinated molybdate group, i.e., Mo^{4+} to Mo^0 and Mo^{6+} to Mo^{4+} [26]. With the increase of carbon loading in catalyst, the TPR peak at low temperature shifts from 481 ºC to 409 ºC. A shoulder peak is observed at 560 ºC for CoMo (C2). It is generally accepted that molybdate has strong interaction with Al_2O_3 support [27]. The shift to lower temperature indicates that interaction between polymolybdate and support decreases with increasing carbon loadings. The shoulder at 560 ºC in CoMo(C2) may represent the intermediate species between tetrahedral and octahedral Mo species. The high asymmetry of peaks at low temperature in CoMo(C1) and CoMo(C1.5) also suggests the distortion of octahedral polymolybdate.

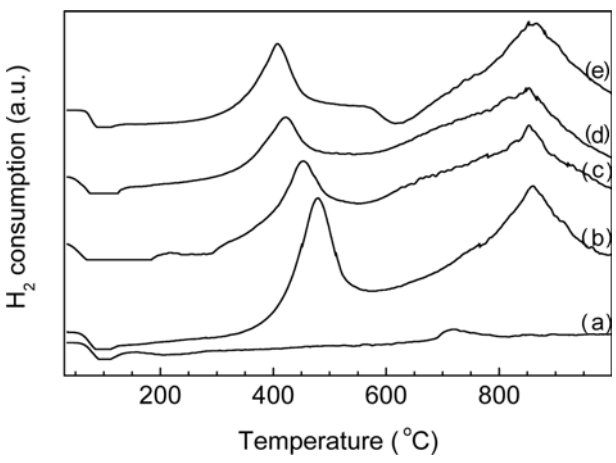

Fig. 3. TPR profiles of (a) γ-Al_2O_3, (b) CoMo(C0), (c) CoMo(C1), (d) CoMo(C1.5) and (e) CoMo(C2).

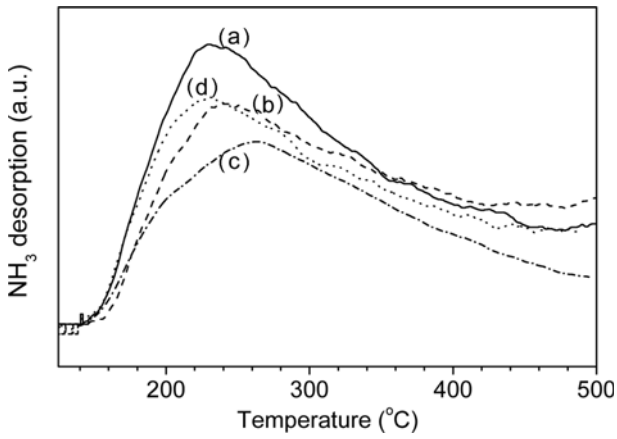

Fig. 4. NH_3-TPD profiles of (a) CoMo(C0), (b) CoMo(C1), (c) CoMo (C1.5) and (d) CoMo(C2).

4. NH_3-TPD

The position and peak area in NH_3-TPD profiles correspond to the intensity of acidity and the number of acid centers, respectively [28]. As shown in Fig. 4, the number of acid centers decreases after introduction of carbon. This can be ascribed to the coverage of acid centers by carbonaceous species. The acid center number in catalyst decreases first with increasing carbon loading, reaches the lowest one for catalyst CoMo(C1.5), and increases afterwards with further increasing the carbon content. Kiviat and Petakis [29] reported that the number of Brønsted (B) acid sites increases apparently after Al_2O_3 impregnated with MoO_3. The B acid sites may originate from Mo-OH groups in polymolybdate. From the TPR results, the carbonaceous species may distort the polymolybdate molecules; this can enhance the intra-molecular strain and weaken the bond of Mo-O-Mo to produce Mo-OH groups. For this reason, the excessive carbon addition may create more acid centers in CoMo(2) catalyst.

5. Sulfidation by Thiophene

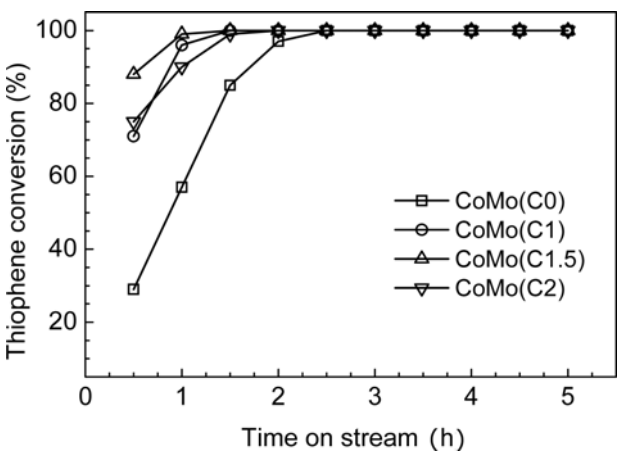

Fig. 5. Conversion of thiophene versus time on stream during sulfidation under 290 ºC, 1.2 MPa, LHSV=8.6 h^{-1}, V(H_2)/V(oil) =140.

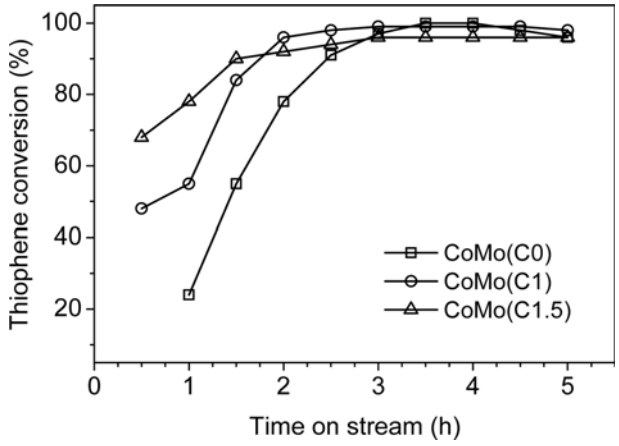

Fig. 6. Conversion of thiophene versus time on stream during sulfidation with a pyridine-containing feed under 290 °C, 1.2 MPa, LHSV=8.6 h^{-1}, $V(H_2)/V(oil)$=140.

The thiophene conversion during the catalyst sulfidation by thiophene is shown in Fig. 5. The initial activity of sulfidation follows the sequence of CoMo(1.5)>CoMo(1)>CoMo(2)>CoMo(0). After about 2.5 h, the thiophene conversion over all the catalysts arrives at 100%. The introduction of carbon species accelerates the sulfidation of catalysts. However, the degree of acceleration drops with excessive carbon addition. From the discussion above, the carbon species in catalysts can be mainly differentiated as intermediate support carbon and coke-like carbon. The intermediate support carbon species are expected to facilitate the sulfidation of active metals owing to decreasing the interaction between active metals and support, while the coke-like carbon species may inhibit the sulfidation of Mo and Co cations due to covering the active metals. In CoMo(C1) and CoMo(1.5), the carbon species as intermediate support may play the dominant role; whereas the influence of coke-like carbon species becomes apparent in CoMo(C2).

6. Effects of Pyridine and Cyclohexene on Catalyst Sulfidation

To examine the influence of any N-containing compounds in the sulfiding feed on the sulfidation of HDS catalyst, pyridine as a model compound was added into thiophene sulfiding feed. As shown in Fig. 6, the addition of pyridine decreased the conversion of thiophene. However, the initial activity of sulfidation still follows the sequence of CoMo(C1.5)>CoMo(C1)>CoMo(C0). This suggests that carbon-containing catalysts can also be sulfided better than carbon-free catalyst with N-containing compounds in the feed.

Olefins as impurities are also usually present in the sulfiding feeds. With addition of cyclohexene in the sulfiding feed, the conversions of thiophene and cyclohexene versus time on stream during the sulfidation are shown in Fig. 7. Unexpectedly, the sulfidation of carbon containing catalysts was strongly depressed by cyclohexene. The sequence of thiophene conversion changes into CoMo(C0)> CoMo(C1)>CoMo(C1.5), contrary to that of sulfidation with olefin-free feed.

It is generally accepted that the acid centers induce the polymerization of olefins and bring on the coke deposition. NH_3-TPD results indicate that carbon addition in the catalyst decreases the total acidity. As compared with the carbon-free catalyst, however, the sulfidation of carbon-containing catalyst here is inhibited by cyclo-

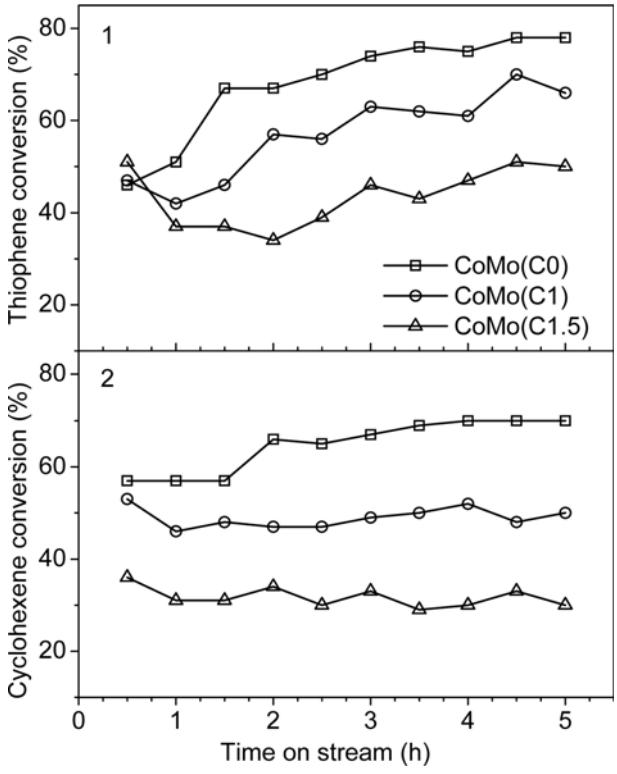

Fig. 7. Effect of cyclohexene on the catalyst sulfidation by thiophene under 320 °C, 1.2 MPa, LHSV=8.6 h^{-1}, $V(H_2)/V(oil)$=140.

hexene. Kiviat and Petakis [29] found that Lewis (L) acid is dominant on the surface of γ-Al_2O_3 support, and B acid increases after impregnation with CoO and MoO_3. In this work, carbonaceous species may distort the polymolybdate molecules to form new B acid sites; these B acid centers may induce the polymerization of olefins, which forms carbonaceous deposit that possibly covers the surface of Mo species. As a result, the sulfidation of catalysts with carbon addition was depressed strongly by cyclohexene. As shown by the tendency of thiophene conversion versus time on stream in Fig. 7, at the beginning of sulfidation, the carbon-containing catalyst even exhibits slightly high thiophene conversion than the carbon-free catalysts. With the accumulation of carbon deposit in catalyst due to the extension of the sulfidation process, the sulfidation of carbon-containing catalyst is then depressed.

The evolution of cyclohexene conversion is similar in sequence to that of thiophene conversion, e.g., CoMo(C0)>CoMo(C1)>CoMo (C1.5). The conversion of cyclohexene reflects the hydrogenation activities of catalysts. The active sites of hydrogenation and desulfurization were suggested to be located at different positions in active phase. Daage et al. proposed that hydrogenation only occurs at the edge of top and bottom layers in multi-layer hexagon MoS_2 crystallites and desulfurization goes at the edges of all layers [30]. Recent observation of scanning tunneling microscopy showed that the sites of hydrogenation in fact are located at the "brim" region in base plane near the edge (Fig. 8). This "brim" has metal-like properties [31]. The conversions of thiophene and cyclohexene decrease simultaneously over carbon-containing catalysts at start stage; however, the conversion of thiophene increases again with prolonging the sulfidation, whereas hydrogenation activities remain constant.

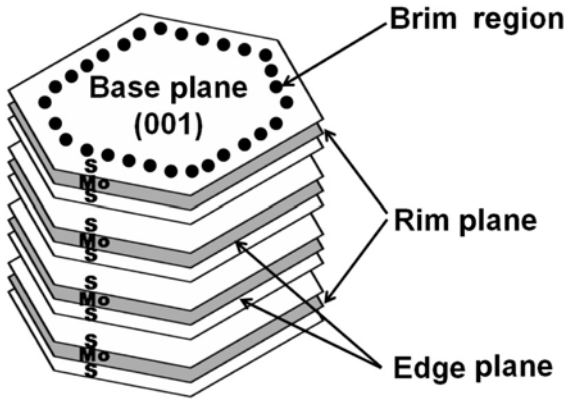

Fig. 8. Scheme of MoS_2 active phase.

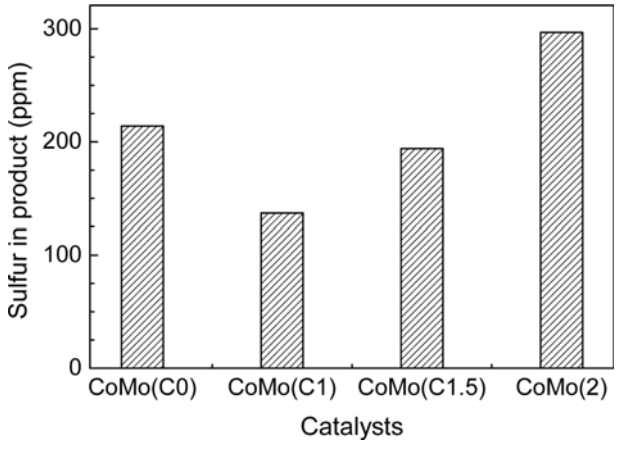

Fig. 9. HDS efficiency over carbon bearing and carbon-free catalysts. Reaction conditions: 290 °C, 1.2 MPa, LHSV=8.6 h^{-1}, $V(H_2)/V(oil)=140$.

We suggest that the coke-like carbon species is more favorable to cover on a base plane than on edge plane. Therefore, the hydrogenation activity was inhibited more than HDS activity. These suggest that carbon-containing catalysts should avoid contacting with olefins during their sulfidation.

7. HDS Activity

The HDS tests of FCC naphtha (containing 866 ppm sulfur) were performed over carbon-containing catalysts and carbon-free catalyst. The catalysts were sulfided by 4.5 vol% H_2S in H_2. As shown in Fig. 9, the carbon-bearing catalysts CoMo(C1) and CoMo(C1.5) exhibit higher activity than carbon-free catalyst; whereas the CoMo (C2) shows lower activity than CoMo(C0). The results illustrate that proper incorporation of carbon in $CoMo/Al_2O_3$ can improve its HDS performance.

CONCLUSIONS

The effects of carbon addition on CoMo catalyst performance for sulfidation and hydrodesulfurization (HDS) were investigated. The results indicate that the incorporation of proper carbon on CoMo catalyst can improve its HDS performance.

Two forms of carbon species were differentiated: one is spread over the catalyst surface, similar to coke formed from reaction; the other interacts with active phase as an intermediate support. The carbon species acting as intermediate support may decrease the interaction of active metals with support, which enhances the sulfidation and HDS activities of CoMo catalyst. However, the coke-like carbon inhibits the sulfidation as well as HDS activities.

The forms of carbon species become complicated with excessive carbon loadings. The carbon species as intermediate support may distort the polymolybdate species to form new B acid sites, which induces the polymerization of olefins and leads to the inhibition of sulfidation.

ACKNOWLEDGMENTS

The authors are grateful for the financial support of the State Key Fundamental Research Project (2006CB202504) and the National Natural Science Foundation of China (No. 20676140, 20873174) and Natural Science Foundation of Shanxi Province of China.

REFERENCES

1. C. Song, *Catal. Today*, **86**, 211 (2003).
2. W. Min, *Korean J. Chem. Eng.*, **19**, 601 (2002).
3. C. Kwak and S. H. Moon, *Korean J. Chem. Eng.*, **16**, 608 (1999).
4. M. C. Kim and K. L. Kim, *Korean J. Chem. Eng.*, **13**, 1 (1996).
5. S. K. Song and S. K. Ihm, *Korean J. Chem. Eng.*, **20**, 284 (2003).
6. H. Hallie, *Oil Gas J.*, **80**, 69 (1982).
7. R. Prada Silvy, P. Grange, F. Delannay and B. Delmon, *Appl. Catal.*, **113**, 46 (1989).
8. R. Prada Silvy, P. Grange and B. Delmon, *Stud. Surf. Sci. Catal.*, **233**, 53 (1989).
9. R. R. Chianelli and G. Berhault, *Catal. Today*, **53**, 357 (1999).
10. X. D. Wen, Z. Cao, Y. W. Li, J. Wang and H. Jiao, *J. Phys. Chem. B*, **110**, 13860 (2006).
11. S. Texier, G. Berhault, G. Pérot, V. Harlé and F. Diehl, *J. Catal.*, **223**, 404 (2004).
12. M. Kouzu, Y. Kuriki, F. Hamdy, K. Sakanishi, Y. Sugimoto and I. Saito, *Appl. Catal. A*, **265**, 61 (2004).
13. L. Kaluža and M. Zdražil, *Carbon*, **39**, 2023 (2001).
14. S. J. Moon and S. K. Ihm, *Korean J. Chem. Eng.*, **11**, 111 (1994).
15. J. P. R. Vissers, B. Scheffer, V. H. J. de Beer, J. A. Moulijn and R. Prins, *J. Catal.*, **105**, 277 (1987).
16. C. Glasson, C. Geantet, M. Lacroix, F. Labruyère and P. Dufresne, *J. Catal.*, **212**, 76 (2002).
17. G. Alonso, G. Berhault, A. Aguilar, V. Collins, C. Ornelas, S. Fuentes and R. R. Chianelli, *J. Catal.*, **208**, 359 (2002).
18. L. Alvarez, J. Espino, C. Ornelas, J. L. Rico, M. T. Cortez, G. Berhault and G. Alonso, *J. Mol. Catal. A*, **210**, 105 (2004).
19. E. Furimsky and F. E. Massoth, *Catal. Today*, **52**, 381 (1999).
20. R. H. Taylor, C. Winbo, G. D. Christian and J. Růžička, *Talanta*, **39**, 789 (1992).
21. Z. B. Wei, W. Yan, H. Zhang, T. Ren, Q. Xin and Z. Li, *Appl. Catal. A*, **167**, 39 (1998).
22. H. K. Matralis, Ch. Papadopoulou and A. Lycourghiotis, *Appl. Catal. A*, **116**, 221 (1994).
23. A. Duan, G. Wan, Z. Zhao, C. Xu, Y. Zheng, Y. Zhang, T. Dou, X. Bao and K. Chung, *Catal. Today*, **119**, 13 (2007).

24. Y. Ch. Park and H.-K. Rhee, *Korean J. Chem. Eng.*, **15**, 411 (1998).
25. V. L. Parola, G. Deganello and A. M. Venezia. *J. Colloid Interface Sci.*, **274**, 159 (2004).
26. D. Ferdous, A. K. Dalai and J. Adjaye, *Appl. Catal. A*, **260**, 137 (2004).
27. B. Hinnemann, J. K. Nørskov and H. Topsøe, *J. Phys. Chem. B*, **109**, 2245 (2005).
28. X. Li, X. Zhang and S. Ge, *J. Fuel Chem. Technol*., **26**, 145 (1998).
29. F. E. Kiviat and L. Petakis, *J. Phys. Chem.*, **77**, 1232 (1973).
30. M. Daage and R. R. Chianelli, *J. Catal.*, **149**, 414 (1994).
31. J. V. Lauritsen, M. Nyberg, J. K. Nørskov, B. S. Clausen, H. Topsøe, E. Lægsgaard and F. Besenbacher, *J. Catal.*, **224**, 94 (2004).